Superluminal tunneling of an electromagnetic *X* wave through a planar slab

Amr M. Shaarawi*
Physics Department, The American University in Cairo, P.O. Box 2511, Cairo 11511, Egypt

Ioannis M. Besieris
The Bradley Department of Electrical and Computer Engineering, Virginia Polytechnic Institute and State University, Blacksburg, Virginia 24061

(Received 18 April 2000)

A study is provided of an *X* wave undergoing frustrated total internal reflection on the upper surface of a planar slab separating two dielectric media. It is shown that the peak of the field transferred through the slab appears to be transmitted at an ultrafast speed. A general analytic solution is derived and is supported by specific numerical examples that indicate that the transport speed of the peak of the *X* wave can be much larger than the speed of light.

PACS number(s): 41.20.Jb, 73.40.Gk, 84.40.Az

I. INTRODUCTION

Recently, the study of pulses tunneling through barriers has attracted considerable attention. It has been demonstrated that the time taken by a pulse to tunnel through a barrier saturates to a constant value as the thickness of the barrier increases [1–4]. This causes the transmission speed of the pulse tunneling through the barrier region to appear to be superluminal. Although tunneling was originally established as a quantum phenomenon, recent experiments demonstrate that classical tunneling can take place. This is usually done by transmitting classical pulses through undersized sections of waveguides [5–14], or by arranging for optical tunneling associated with frustrated total internal reflection [15,16]. Similar results are also obtained for photons tunneling through dielectric mirrors [17,18]. The apparent superluminal character of the tunneling pulses has initiated a spirited debate about the interpretation of the tunneling time [19–30] and experiments have been performed to determine the accuracy for different criteria set to define such time [16]. It is worthwhile to stress the fact that it has been established that the peak of the tunneling pulse is not causally related to that of the incident one. Energy flow analysis shows that the main contribution to the transmitted field comes from the leading portion of the tunneling pulse [4,23]. This causes a new peak to form in that leading part of the pulse, which is not causally related to the portion of the field containing the peak of the incident pulse. This reshaping of the transmitted waveform is the reason for the apparent superluminal propagation.

In this paper, we study the case of frustrated total internal reflection of a three-dimensional classical pulse, namely, the *X* wave [31–35]. The *X* wave is synthesized from a superposition of polychromatic plane-wave components having wave vectors restricted to a conic surface [36,37]. The *X* wave is a dispersion free localized pulse that travels in free space without spreading out. For the setup shown in Fig. 1, the *X* wave is normally incident on the interface separating regions I and II that have refractive indices n_1 and n_2, respectively. If the apex angle ξ of the spectral conic surface characterizing the *X* wave is chosen to be larger than the critical angle $\theta_c = \sin^{-1}(n_2/n_1)$, then the spectral plane-wave components of the *X* wave undergoes total internal reflection. Consequently, frustrated total internal reflection takes place and evanescent fields are generated in region II. For a thin slab, the evanescent fields mediate the transmission of the *X* wave into region III. In this paper, we are primarily interested in the behavior of the transmitted *X* wave. We demonstrate that the time taken by the *X* wave to tunnel through a thin barrier saturates as the barrier thickness increases. It is shown that an increase in the barrier thickness causes the central portion of the transmitted pulse to enlarge in addition to the expected decrease in the amplitude of the tunneling *X* wave. One should note, however, that the ''fattened'' *X* wave transmitted into region III is still dispersion free and does not spread out as it travels away from the slab.

A simple analytical solution is obtained for the tunneling of a three-dimensional *X* wave through a planar slab. The deduced results explicitly represent the tunneling of a classical electromagnetic pulse in $(3+1)$ space-time dimensions. This eliminates unrealistic effects arising in one- or two-dimensional analyses, e.g., the unrealistic long tails associated with two-dimensional (2D) pulses [38]. Moreover, the 3D analysis allows us to study the effect of tunneling on both the axial and lateral widths of the transmitted pulse. The current investigation is geared towards the study of the time taken by the peak of an *X* wave to tunnel through slabs of different widths. Furthermore, this investigation complements other studies of the behavior of the reflection and transmission of *X* waves from planar multilayered media [39–41]. This paper aims at making use of the extended focus depth of the *X* waves and their ultrawideband spectral content in applications involving high-resolution imaging and detection of buried objects.

The plan of this paper is to solve for the field of an *X* wave transmitted through a planar slab. This is done in Sec.

*Permanent address: Department of Engineering Physics and Mathematics, Faculty of Engineering, Cairo University, Giza 12211, Egypt.

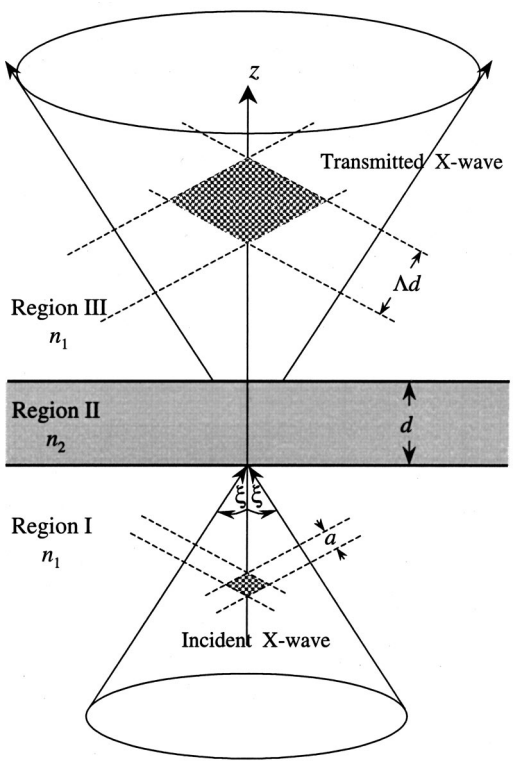

FIG. 1. The *X* wave incident normally on the upper surface of the slab. The *X* wave can be viewed as pulsed plane waves traveling along a conic surface having apex angle ξ. The axial width of the incident (transmitted) pulse is proportional to $a(\Lambda d)$. The region of intersection of the pulsed fields yields the peaked portion of the field of the *X* wave. The darkened areas in the diagram indicate that the transmitted pulse acquires axial and lateral widths larger than those of the incident pulse.

II where we consider the case of normal incidence for which all spectral components of the *X* wave undergo frustrated total internal reflection. In Sec. III, we present specific numerical results. Concluding remarks are provided in Sec. IV

II. ANALYSIS

Consider the schematic representation of the *X* wave given in Fig. 1. The apex angle of the conic surface defining the wave vectors associated with the spectral plane-wave components of the *X* wave is chosen so that $\xi > \theta_c = \sin^{-1}(n_2/n_1)$. For propagation along the positive *z* direction, transverse electric (TE) polarization of the plane-wave components of the *X* wave is achieved by working with the following vector Hertzian potential [42]:

$$\vec{\Pi}_{\mathrm{TE}}(\vec{r},t) = \Psi(\vec{r},t)\vec{u}_z . \tag{1a}$$

The electric-field intensity can be readily obtained, viz.,

$$\vec{E}(\vec{r},t) = -Z_0 \vec{\nabla} \times \partial_{ct} \vec{\Pi}_{\mathrm{TE}}(\vec{r},t), \tag{1b}$$

where $Z_0 = \sqrt{\mu_0/\varepsilon_0}$, assuming that the medium is nonmagnetic. For an *X* wave normally incident on the slab, the Hertzian potential is defined in terms of a fourfold Fourier superposition as

$$\Psi^{(i)}(\vec{r},t) = \int_{R^1} d(\omega/c_1) \int_{R^3} d^3\vec{k} A(\vec{k},\omega) \times e^{-i\omega t} e^{+i(k_x x + k_y + k_z z)} \delta[(\omega/c_1)^2 - k_x^2 - k_y^2 - k_z^2], \tag{2a}$$

where $c_1 = c_0/n_1$ is the wave speed in region I and the spectral amplitude is given by

$$A(\vec{k},\omega) = \frac{1}{\pi}(\omega/\omega_0)^{\mu} e^{-(\omega/c_1)a} \delta[k_z - (\omega/c_1)\cos\xi], \quad a > 0. \tag{2b}$$

The integrations in Eq. (2a) can be carried out explicitly to give the μth order scalar *X* wave solution; specifically,

$$\Psi^{(i)}(\vec{r},t) = \frac{\Gamma(\mu+1)}{(\omega_0/c_1)^{\mu}\sqrt{\{\rho^2\sin^2\xi + [a - i(z\cos\xi - c_1 t)]^2\}^{\mu+1}}} \times F\left(\frac{\mu+1}{2}, -\frac{\mu}{2}, 1, \times \frac{\rho^2\sin^2\xi}{\rho^2\sin^2\xi + [a - i(z\cos\xi - c_1 t)]^2}\right). \tag{3}$$

Here, *F* is the hypergeometric function [43]. For integer values $\mu = m$, the above expression assumes the following form

$$\Psi^{(i)}(\vec{r},t) = (\omega_0/c_1)^{-m} \partial_a^m \times (\{\rho^2\sin^2\xi + [a - i(z\cos\xi - c_1 t)]^2\}^{-1/2}).$$

To determine the Hertzian potential associated with the field transmitted into region III, one has to determine the transmitted plane-wave components contributing to a Fourier superposition similar to the one given in Eq. (2a). For frustrated total internal reflection, the transmission coefficient relating the spectral amplitudes in regions I and III is given by [15,44,45]

$$t(\vec{k},\omega) = \frac{i2Kk_z}{(k_z^2 - K^2)\sinh(Kd) + i2Kk_z\cosh(Kd)}, \tag{4}$$

where $K = (\omega/c_1)\sqrt{\sin^2\xi - n_{21}^2} = (\omega/c_1)\Lambda$ and $n_{21} = n_2/n_1$. Furthermore, we have used the definition of apex angles of the *X* wave vectors $\vec{k}$ to substitute $\sin\theta_k = \sin\xi$ in the expression for *K*. The Hertzian potential associated with the transmitted field acquires the following form:

$$\Psi^{(t)}(\vec{r},t) = \int_{R^t} d(\omega/c_1) \int_{R^3} d^3\vec{k} t(\vec{k},\omega) A(\vec{k},\omega) \times e^{-i\omega t} e^{+i[k_x x + k_y y + k_z(z-d)]} \times \delta[(\omega/c_1)^2 - k_x^2 - k_y^2 - k_z^2]. \tag{5}$$

The three integrations over $\vec{k}$ are carried out analytically to give

$$\Psi^{(t)}(\vec{r},t)=\int_0^\infty d(\omega/c_1)(\omega/\omega_0)^\mu J_0[(\omega/c_1)\rho\sin\xi]e^{-(\omega/c_1)\{a-i[(z-d)\cos\xi-c_1t]}\times\frac{i2\Lambda\cos\xi}{(\cos^2\xi-\Lambda^2)\sinh[(\omega/c_1)\Lambda d]+i2\Lambda\cos\xi\cosh[(\omega/c_1)\Lambda d]}. \quad (6)$$

One should note that for $(\omega/c_1)\Lambda d\gg 1$, the two terms $\sinh[(\omega/c_1)\Lambda d]$ and $\cosh[(\omega/c_1)\Lambda d]$ are approximately equal to $0.5\exp[(\omega/c_1)\Lambda d]$. If most of the significant spectral components contributing to the integrand in Eq. (6) obey this condition, the integration can be performed analytically [cf., Eq. (6.621.1) in Ref. [43]] to give the following approximate expression:

$$\Psi^{(t)}(\vec{r},t)\cong\frac{i4\Gamma(\mu+1)\Lambda\cos\xi}{(\omega_0/c_1)^\mu(\cos^2\xi-\Lambda^2+i2\Lambda\cos\xi)\sqrt{(\rho^2\sin^2\xi+\{a+\Lambda d-i[(z-d)\cos\xi-c_1t]\}^2)^{\mu+1}}}\times F\left(\frac{\mu+1}{2},-\frac{\mu}{2},1,\frac{\rho^2\sin^2\xi}{\rho^2\sin^2\xi+\{a+\Lambda d-i[(z-d)\cos\xi-c_1t]\}^2}\right). \quad (7)$$

For barrier thickness satisfying $\Lambda d>a$, the axial and lateral widths are determined by Λd instead of a. Consequently, the transmitted pulse acquires lateral and axial widths that are larger than those exhibited by the incident field. This result is confirmed in the next section where specific numerical examples are considered. Another interesting feature inferred from the expression given in Eq. (7) is that the ratio between the amplitudes of the peaks of the incident and transmitted pulses is equal to $(a/\Lambda d)^{\mu+1}$. Consequently, the decay in the peak of the pulse traversing the tunneling region varies algebraically with the width of the slab. This should be contrasted with the common view that evanescent fields lead to exponentially fast roll off in the tunneling region. For the X wave, the amplitude of the transmitted pulse starts falling off quickly when Λd becomes comparable to a. Any further increase in the width of the slab causes small changes in the amplitude of the peak of the transmitted pulse. This could allow for ultrafast transmission over extended tunneling distances.

III. NUMERICAL RESULTS

Consider the case of an X wave normally incident on the interface separating the two regions I and II, for which $n_1=1.3$ and $n_2=1.0$. The X wave is characterized by the apex angle $\xi=51°$, and the parameter $a=0.05$ m. Note that $\xi>\sin^{-1}$ and $n_{21}=50.285°$; thus, the spectral plane-wave components of the X wave will undergo frustrated total internal reflection. A surface plot of the incident X wave is provided in Fig. 2 at $c_1t=-50$ m. For the pulse shown in Fig. 2, we have used $\mu=1/2$ and $(\omega_0/c_1)=1/a$. In Fig. 3, we display the pulse transmitted through a slab of width $d=0.2$ m. The figure confirms the predicted ''fattening'' of the transmitted pulse. This ''fattened'' pulse propagates in region III without any further spreading out, i.e., the transmitted pulse retains its localized character while propagating in region III. Furthermore, one should note that the peak of the pulse is shifted forward relative to the rest of its field. In order to clarify this point, we compare in Fig. 4 plots of the axial profiles of the transmitted pulses for $d=0$ and $d=0.2$ m. The former corresponds to the case of having no slab, or to that of an X wave propagating in a continuous medium having refractive index n_1. The peak of such an X wave is positioned at z_0 and that of the tunneling X wave is found at z_m. As can be seen from Fig. 4, the peak of the pulse transmitted through the slab is located in front of the peak of the pulse traveling in the dielectric material. This behavior is due to the reshaping of the pulse in the evanescent-field or tunneling region. If one is only interested in the peaked regions of the field, then the pulse appears to have traveled at a superluminal speed inside the tunneling region. In Fig. 5, we compare the axial profile of the free-space X wave to a tunneling pulse with $a=0.01$ m. The same behavior illustrated in Fig. 4 is seen, however, the decay of the amplitude of the tunneling pulse is greater. This faster decay can be explained by the fact that larger bandwidths correspond to smaller values of a. Thus, the cutoff introduced by the $\exp[-(\omega/c_1)\Lambda d]$ factor arising from the transmission coefficient removes larger portions of the spectrum when a is small. This establishes the fact that the decrease in

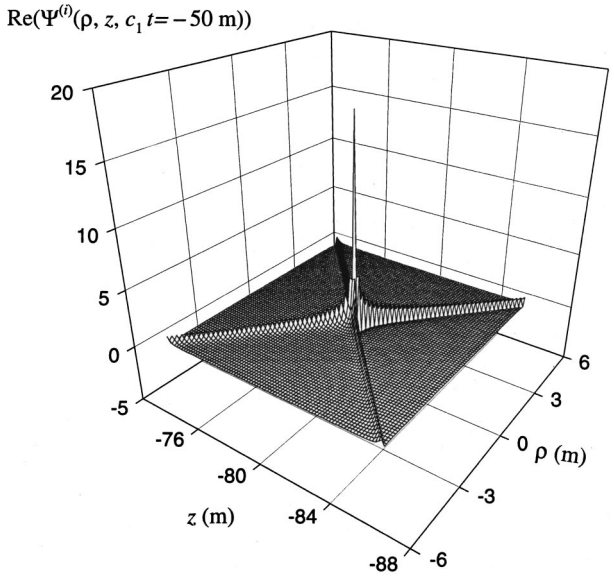

FIG. 2. Surface plot of the incident X wave evaluated at $c_1t=-50$ m. The X wave pulse has $a=0.05$ m, $\xi=51°$, $\mu=0.5$, and $(\omega_0/c_1)=20\,\mathrm{m}^{-1}$.

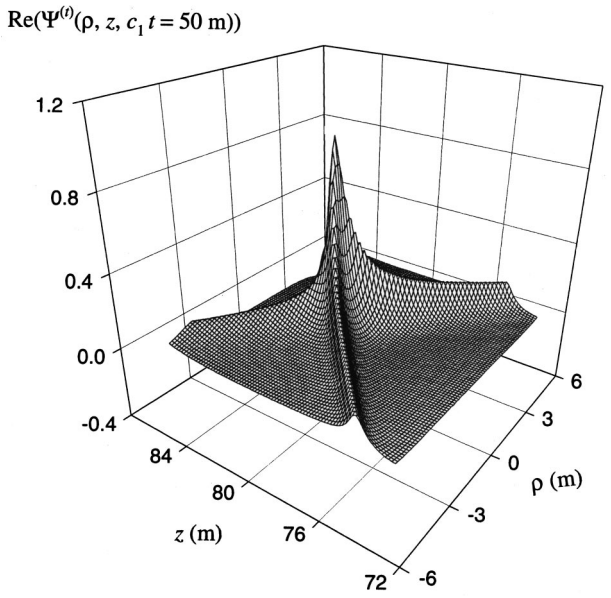

FIG. 3. Surface plot of the transmitted X wave field evaluated at $c_1 t = 50$ m. The incident X wave is the same one shown in Fig. 2. The slab width is $d = 2$ m and the refractive indices are $n_1 = 1.3$ and $n_2 = 1$.

the amplitude of the transmitted pulse depends on the magnitude of a in comparison to Λd.

In order to quantify the results discussed in the preceding paragraph, we proceed with the following approximate analysis. We assume that the propagation of the transmitted pulse in region III is constant and is equal to $c_1/\cos\xi$. At time t, the peak of the pulse reaches point z_m after tunneling through a slab of thickness d. The tunneling time τ can be

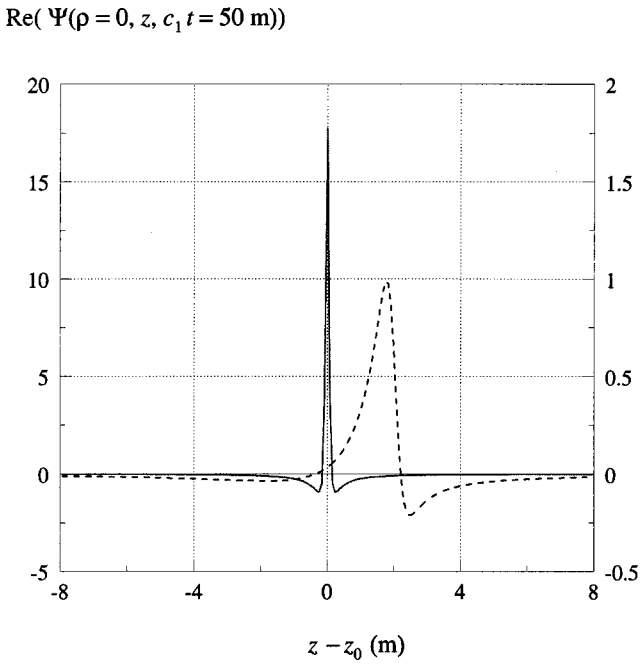

FIG. 4. The axial profiles of the amplitudes of transmitted pulses for $d = 0$ (solid line) and $d = 0.2$ m (broken line). The two profiles were evaluated for $a = 0.05$ m. The right (left) axis represents the amplitude of the pulse for $d = 0.2$ m ($d = 0$).

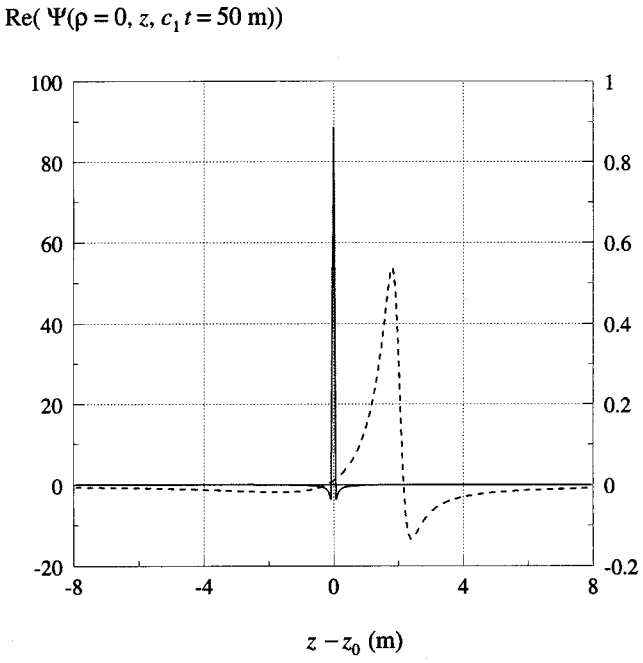

FIG. 5. The axial profiles of the amplitudes of transmitted pulses for $d = 0$ (solid line) and $d = 0.2$ m (broken line). The two profiles were evaluated for $a = 0.01$ m. The right (left) axis represents the amplitude of the pulse for $d = 0.2$ m ($d = 0$).

evaluated by using the following simple expression:

$$c_1\tau = c_1 t - (z_m - d)\cos\xi. \tag{8}$$

Consequently, the tunneling speed assumes the following form:

$$(v_{\text{tun}}/c_1) = \frac{d}{c_1 t - (z_m - d)\cos\xi}. \tag{9}$$

To have a feeling of how fast the peak of the X wave is transmitted through the slab, we have plotted the difference $(z_m - z_0) - d$ for different values of d. The quantity $(z_m - z_0)$ is the forward displacement of the peak for a thickness of the slab equal to d. The difference $(z_m - z_0) - d$ thus provides an estimate of the amount of forward displacement of the peak of the X wave relative to the width of the slab. Obviously, a zero difference suggests that the tunneling speed of the peak of the pulse appears to be infinite. On the contrary, very small differences compared to d indicate ultrafast transmission through the slab. The plots in Fig. 6 show that the forward shift in the position of the peak of the transmitted X wave is almost equal to the width of the slab. Since the speed of the peak in region III is constant, the results, illustrated in Fig. 6, indicate that the forward shift occurred in the region of the slab through which transmission is extremely fast. The negative values of the difference $(z_m - z_0) - d$ show that the tunneling time is very short but not equal to zero. Furthermore, one should observe that the shift in the position of the peak is larger for $a = 0.01$ m. This is the case because $a/\sin\xi$ determines the axial width. Therefore, a slab having a specific thickness would appear wider for a pulse having a shorter axial width.

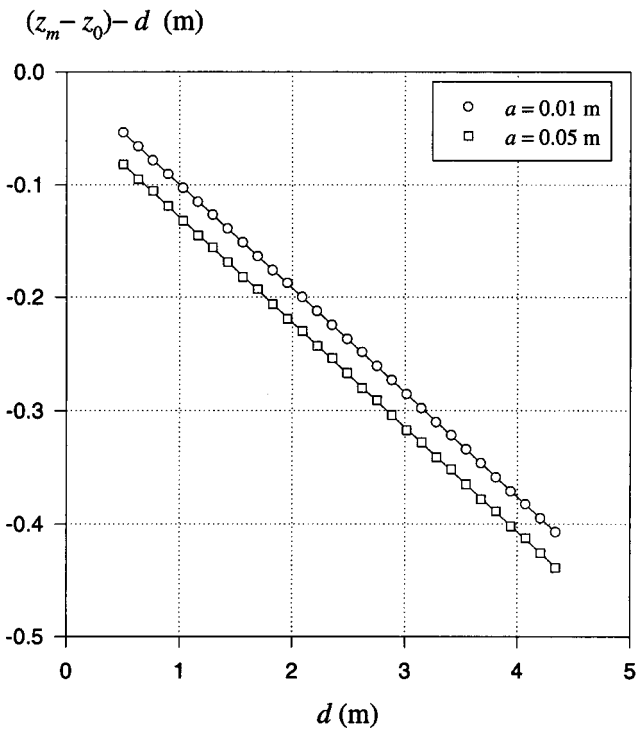

FIG. 6. Plots of the difference $(z_m - z_0) - d$ vs the slab width d. The quantity $(z_m - z_0)$ is the amount of forward displacement of the peak for a specific slab thickness d. The difference $(z_m - z_0) - d$ provides an estimate of the amount of forward displacement of the peak of the X wave relative to the width of the slab.

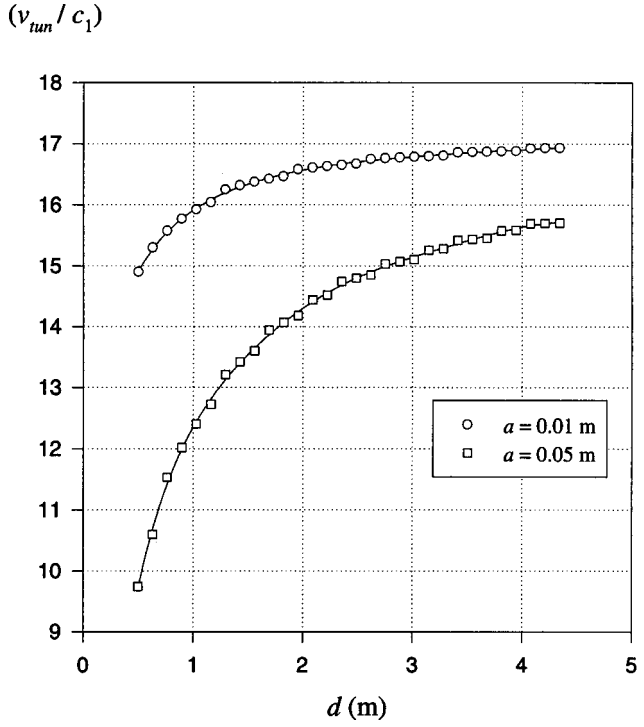

FIG. 7. Plots of the tunneling velocity (v_{tun}/c_1) vs the slab width d. The solid lines represent cubic regressions of the calculated velocities.

The preceding argument is supported by evaluating the tunneling velocity given in Eq. (9) for $a = 0.01$ and 0.05 m. In Fig. 7, we provide plots of the tunneling velocity v_{tun}/c_1 versus the slab width d. The speed of transmission of the peak of the pulse through the slab appears to be 10–17 times faster than $c_1 = c_0/n_1$. The tunneling speed of a pulse having $a = 0.01$ m is higher than that of an X wave having $a = 0.05$ m. The reason for this is that for a fixed ξ value there are only two length scales, namely, the width of the slab d and the size of the peaked portion of the X wave determined by a. For a smaller a, the slab appears to be wider. As such, the plot for $a = 0.01$ m would be similar to that corresponding to $a = 0.05$ m calculated for slabs that were 5-times wider. In Fig. 7, the solid lines represent cubic regressions of the velocities calculated using the numerically evaluated discrete positions of the peaks. The irregularity in the distribution of the various points are due to errors introduced by the computed discrete positions of the peaks that are slightly different from their real locations.

Finally, we would like to comment on the origin of the fast transmission of the peak of the X wave in the tunneling region. It is well established that the peak of an X wave traveling in free space is superluminal [31–33]. For example, the parameters chosen in the previous examples give $v_1 = c_0/n_1 \cos\xi = 1.22c_0$. The superluminality of the peaks of the X waves arise from the interference of plane waves propagating along wave vectors situated on a conical surface. The plane-wave components of the X wave travel at the speed of light, while the speed of their interference peak is superluminal. This superluminal speed is directly related to the apex angle of the cone ξ. For a cone angle $\xi \sim \pi/2$, the speed of the peak of an X wave approaches ∞. At this stage, we should recall that the evanescent fields generated on an interface separating two semi-infinite regions propagate in directions parallel to the interface and do not have components normal to it [39]. For an X wave, these components traveling parallel to the interface correspond to a flat cone having $\xi = \pi/2$. Nonetheless, infinite speed of transmission is not observed in this situation because the width of the second region is infinite. For a slab of finite width, frustrated transmission occurs through region II. In order for that transmission to take place, there should be a small but finite-energy transfer in the direction normal to the interface. Within such a framework, the evanescent fields can be perceived as traveling at very small grazing angles to the interface. These angles become smaller and approach zero as the width of region II is increased. In region II, the spectral cone of an X wave undergoing frustrated total internal reflection would thus have an effective angle $\xi_{\text{eff}} \sim \pi/2$ in region II. Figure 8 shows that this effective angle gets closer to $\pi/2$ as the width of the slab is increased. Hence, the effective speed of transmission through region II increases for wider slabs and can be several times as fast as the speed of light in vacuum. This picture provides an interesting qualitative explanation of the extremely fast superluminal transmission of the peak of an X wave undergoing frustrated total internal reflection. However, one must emphasize that ξ_{eff} is a mere construction because the evanescent field components are not represented by homogeneous plane waves propagating in the z direction.

IV. CONCLUDING REMARKS

We have studied the transmission of a three-dimensional X wave undergoing frustrated total internal reflection. To the

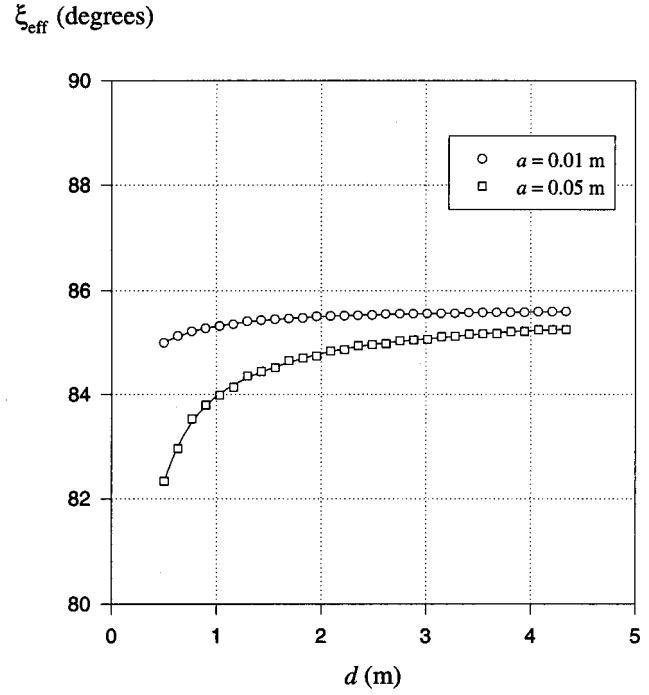

FIG. 8. Plots of the effective apex angle inside the slab ξ_{eff} vs the slab width d. The solid lines represent cubic regressions of the calculated angles.

best of our knowledge, this is the first three-dimensional analysis of this kind. The results of our calculations simulate accurately the behavior of classical pulses tunneling through planar slabs. Realistic outcomes like the ''fattening'' of the transmitted pulse could have been obscured in two- and one-dimensional studies. We have demonstrated that a tunneling X wave would effectively be transmitted through region II at speeds that can reach several times the speed of light in vacuum. The results of this paper are quite general and the same analysis is applicable to any pulses or beams whose spectral components have wave vectors confined to conic surfaces, e.g., focus wave modes, and Bessel beams [33,46–49]. Optical sources capable of generating X waves, as well as other similar wave fields, have been reported [50–53]. This makes it possible to test experimentally the predictions of the analysis presented in this paper. Experimental difficulties arise due to the large ξ angle needed for the incident field. However, this difficulty might be circumvented by using obliquely incident X waves having smaller ξ angles. Calculations of tunneling speeds of obliquely incident pulses must nonetheless be carried out before one can assert that similar results will be obtained.

There have been claims that the existence of superluminal X waves or of superluminally tunneling pulses, contradicts the theory of special relativity. One should be careful with such assertions because it appears that superluminality is associated only with the peaks of an extended wave field structure. The forward shift of such peaks within the distribution of the whole wave field does not violate special relativity as long as the wave front of the total field is moving at the speed of light. Another point that needs to be clarified before jumping into premature conclusions is the time dependence of the buildup of evanescent fields in region II. In a previous study of acoustic X waves reflected and transmitted from an interface separating two media, a closed-form expression for the evanescent fields has been deduced [39]. Such an expression shows that the amplitude of the evanescent field exhibits an explicit wave translation in the direction normal to the interface. A similar behavior in the case of a slab is expected although the analysis would be quite involved. Studies of this type should give better insight into the nature of the temporal buildup of evanescent fields.

In this paper, we have emphasized the superluminal behavior of the tunneling X waves. Our analysis has been geared towards the evaluation of the time that the peak of the X wave appears to spend in region II. The results of this paper can be extended in a number of ways. For example, we consider having a dielectric slab with refractive index $n_2 < n_1$. An accurate measurement of the arrival time of the peak of the tunneling X wave gives information about the thickness of the dielectric slab and its relative permittivity. Obviously, we need to send two X waves having different ξ angles in order to determine accurately these two quantities. A similar concept has been investigated in connection to parameter characterization of multilayered media using the reflections of two different X waves [40]. Another possible extension of the current analysis is to study the tunneling of X waves through two slabs separated by a large distance. There have been reports that the transmission speeds of 1D pulses through two barriers is independent not only of their widths but also of the distance between them [54]. This can produce extremely fast transmission speeds much larger than the speed of light. It should be of interest to see if the same results hold for 3D X waves.

ACKNOWLEDGMENT

The authors would like to thank E. Recami for continuous scientific collaboration and a productive exchange of ideas.

[1] T. E. Hartman, J. Appl. Phys. **33**, 3427 (1962).
[2] E. H. Hauge and J. A. Støvneng, Rev. Mod. Phys. **61**, 917 (1989).
[3] V. S. Olkhovsky and E. Recami, Phys. Rep. **214**, 339 (1992).
[4] Th. Martin and R. Landauer, Phys. Rev. A **45**, 2611 (1992).
[5] G. Nimtz, A. Enders, and H. Spieker, J. Phys. I **4**, 1 (1994).
[6] A. Enders and G. Nimtz, J. Phys. I **2**, 1693 (1992).
[7] A. Enders and G. Nimtz, Phys. Rev. E **48**, 632 (1993).
[8] A. Enders and G. Nimtz, J. Phys. I **3**, 1089 (1993).
[9] G. Nimtz and W. Heitmann, Prog. Quantum Electron. **21**, 81 (1997).
[10] T. Emig, Phys. Rev. E **54**, 5780 (1996).
[11] H. D. Dahmen, E. Gjonaj, and T. Stroh, Ann. Phys. (Leipzig) **7**, 645 (1998).
[12] R. Landauer and Th. Martin, Rev. Mod. Phys. **66**, 217 (1994).
[13] D. Mugnai, A. Ranfagni, R. Ruggeri, A. Agresti, and E. Recami, Phys. Lett. A **209**, 227 (1995).
[14] J. Jakiel, V. S. Olkhovsky, and E. Recami, Phys. Lett. A **248**, 156 (1998).
[15] A. Ghatak and S. Banerjee, Appl. Opt. **28**, 1960 (1989).

[16] Ph. Balcou and L. Dutraix, Phys. Rev. Lett. **78**, 851 (1997).
[17] A. M. Steinberg, P. G. Kwiat, and R. Y. Chiao, Phys. Rev. Lett. **71**, 708 (1993).
[18] V. Laude and P. Tournois, J. Opt. Soc. Am. B **16**, 194 (1999).
[19] V. S. Olkhovsky, E. Recami, F. Raciti, and A. K. Zaichenko, J. Phys. I **5**, 1351 (1995).
[20] A. Ranfagni, D. Mugnai, and A. Agresti, Phys. Lett. A **158**, 161 (1991).
[21] H. Goenner, Ann. Phys. (Leipzig) **7**, 774 (1998).
[22] J. M. Deutch and F. E. Low, Ann. Phys. (N.Y.) **228**, 184 (1993).
[23] X. Chen and C. Xiong, Ann. Phys. (Leipzig) **7**, 631 (1998).
[24] G. Nimtz, Ann. Phys. (Leipzig) **7**, 618 (1998).
[25] K. Hass and P. Busch, Phys. Lett. A **185**, 9 (1994).
[26] E. Recami, H. E. Hernández F., and A. P. L. Barbero, Ann. Phys. (Leipzig) **7**, 764 (1998).
[27] D. Mugnai, A. Ranfagni, R. Ruggeri, and A. Agresti, Phys. Rev. Lett. **68**, 259 (1992).
[28] K. Imafuku, I. Ohba, and Y. Yamanaka, Phys. Lett. A **204**, 329 (1995).
[29] C. R. Leavens and W. R. Mckinnon, Phys. Lett. A **194**, 12 (1994).
[30] W. Heitmann and G. Nimtz, Phys. Lett. A **196**, 154 (1994).
[31] J. Y. Lu and J. F. Greenleaf, IEEE Trans. Ultrason. Ferroelectr. Freq. Control **39**, 19 (1992).
[32] R. W. Ziolkowski, I. M. Besieris, and A. M. Shaarawi, J. Opt. Soc. Am. A **10**, 75 (1993).
[33] P. Saari and K. Reivelt, Phys. Rev. Lett. **21**, 4135 (1997).
[34] I. M. Besieris, M. Abdel-Rahman, A. Shaarawi, and A. Chatzipetros, *Progress in Electromagnetics Research (PIER)* (EMW Publishing, Cambridge, MA, 1998), Vol. 19, pp. 1.
[35] E. Recami, Physica A **252**, 586 (1998).
[36] J. Fagerholm, A. T. Friberg, J. Huttunen, D. P. Morgan, and M. M. Salomaa, Phys. Rev. E **54**, 4347 (1996).
[37] A. T. Friberg, J. Fagerholm, and M. M. Salomaa, Opt. Commun. **136**, 207 (1997).
[38] E. Heyman and R. Ianconescu, IEEE Trans. Antennas Propag. **AP-38**, 1791 (1990).
[39] A. M. Shaarawi, I. M. Besieris, A. M. Attiya, and E. El-Diwany, J. Acoust. Soc. Am. **107**, 70 (2000).
[40] A. M. Attiya, E. A. El-Diwany, A. M. Shaarawi, and I. M. Besieris, *Progress in Electromagnetics Research (PIER)*, Ref. [34], Vol. 30, p. 191.
[41] A. M. Shaarawi, I. M. Besieris, A. M. Attiya, and E. A. El-Diwany, *Progress in Electromagnetics Research (PIER)*, Ref. [34], Vol. 30, p. 215.
[42] J. A. Stratton, *Electromagnetic Theory* (McGraw Hill, New York, 1941).
[43] I. S. Gradshteyn and I. M. Ryzhik, *Tables of Integrals, Series and Products* (Academic, NY, 1965).
[44] M. Born and E. Wolf, *Principles of Optics* (Pergamon, Oxford, 1989).
[45] B. A. Raad and I. Jacob, IEEE Trans. Educ. **35**, 112 (1992).
[46] J. N. Brittingham, J. Appl. Phys. **54**, 1179 (1983).
[47] R. W. Ziolkowski, J. Math. Phys. **26**, 861 (1985).
[48] P. Hillion, Opt. Commun. **153**, 199 (1998).
[49] A. M. Shaarawi, J. Opt. Soc. Am. A **14**, 1804 (1997).
[50] P. Saari and H. S̃onajalg, Laser Phys. **7**, 32 (1997).
[51] J. Durnin, J. J. Miceli, Jr., and J. H. Eberly, Phys. Rev. Lett. **58**, 1499 (1987).
[52] J. Turnen, A. Vasara, and A. T. Friberg, Appl. Opt. **27**, 3959 (1988).
[53] Z. L. Horvath, M. Erdelyi, G. Szabo, Zs. Bor, F. K. Tittel, and J. R. Cavallaro, J. Opt. Soc. Am. A **14**, 3009 (1997).
[54] A. P. L. Barbero, H. E. Hernández F., and E. Recami, Lanl Archives No. physics/9811001, Phys. Rev. E. (to be published).